Molecular Crystals and Liquid Crystals Science and Technology. Section A. Molecular Crystals and Liquid Crystals

Publication details, including instructions for authors and subscription information:
http://www.tandfonline.com/loi/gmcl19

Topological Effects on Conductance of Nanotubes

Hajime Matsumura [a] & Tsuneya Ando [a]

[a] Institute for Solid State Physics, University of Tokyo, 7-22-1 Roppongi, Minato-ku, Tokyo, 106-8666, Japan

Version of record first published: 24 Sep 2006

To cite this article: Hajime Matsumura & Tsuneya Ando (2000): Topological Effects on Conductance of Nanotubes, Molecular Crystals and Liquid Crystals Science and Technology. Section A. Molecular Crystals and Liquid Crystals, 340:1, 725-730

To link to this article: http://dx.doi.org/10.1080/10587250008025554

Mol. Cryst. and Liq. Cryst., 2000, Vol. 340, pp. 725-730
Reprints available directly from the publisher
Photocopying permitted by license only

Topological Effects on Conductance of Nanotubes

HAJIME MATSUMURA and TSUNEYA ANDO

Institute for Solid State Physics, University of Tokyo, 7–22–1 Roppongi, Minato-ku, Tokyo 106–8666, Japan

(Received May 30, 1999; In final form July 2, 1999)

Electronic states in junctions of nanotubes with different circumferences are studied in an effective-mass approximation. The junction is characterized by boundary conditions which mix wave functions associated with K and K′ points. At ε=0, they decay linearly with the distance from the thicker nanotube, showing that the conductance decays with the junction length in proportion to its third power.

Keywords: graphite; carbon nanotube; junction; five- and seven-member ring; conductance; effective-mass theory

1. INTRODUCTION

A junction which connects carbon nanotubes (CN's) with different diameters through a region sandwiched by a pentagon-heptagon pair has been observed in the transmission electron microscope.[1] Some theoretical calculations on CN junctions within a tight-binding model were reported, which imply that the conductance of junctions exhibits a universal power-law dependence on the ratio of the circumference of two nanotubes.[2] The purpose of this paper is to clarify electronic states and their topological characteristics in junctions consisting of two nanotubes with different diameters in a $\mathbf{k}\cdot\mathbf{p}$ scheme.

2. EFFECTIVE-MASS DESCRIPTION

In the vicinity of K and K' points of the first Brillouin zone of two-dimensional (2D) graphite, electronic states are described by a four-component envelope function $\mathbf{F} = {}^t(F_A^K, F_B^K, F_A^{K'}, F_B^{K'})$. Here, F_A^K and F_B^K are the envelope functions at A and B site of the graphite, respectively, related to the K point, and $F_A^{K'}$ and $F_B^{K'}$ are those for the K` point. The wave function $\mathbf{F}$ satisfies an equation same as Weyl's equation for neutrinos:[3]

$$\mathcal{H}\mathbf{F}(\mathbf{r}) = \varepsilon\mathbf{F}(\mathbf{r}), \tag{2.1}$$

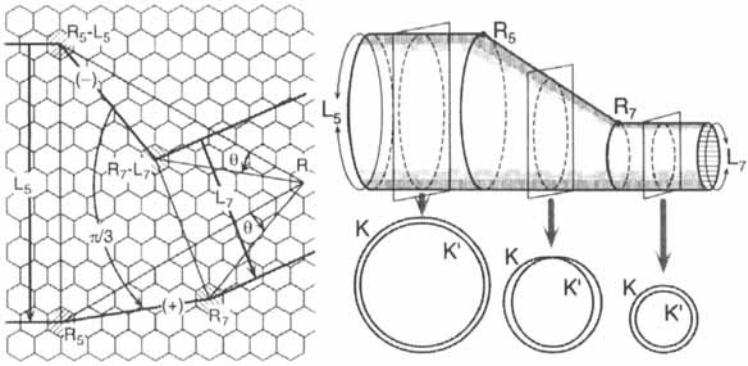

FIGURE 1 (left) The structure of a junction consisting of two nanotubes having an axis not parallel to each other (θ is their angle).

FIGURE 2 (right) Schematic illustration of the topological structure of a junction. In the tube regions, two cylinders corresponding spaces for the K and K' points are independent of each other. In the junction region, they are interconnected to each other.

with

$$\mathcal{H} = \begin{pmatrix} 0 & \gamma(\hat{k}_x - i\hat{k}_y) & 0 & 0 \\ \gamma(\hat{k}_x + i\hat{k}_y) & 0 & 0 & 0 \\ 0 & 0 & 0 & \gamma(\hat{k}_x + i\hat{k}_y) \\ 0 & 0 & \gamma(\hat{k}_x - i\hat{k}_y) & 0 \end{pmatrix}. \tag{2.2}$$

where γ is a band parameter and $\hat{\mathbf{k}} = -i\nabla + (e/c\hbar)\mathbf{A}$. In this paper, we shall study the problems in the absence of a magnetic field only and we set $\mathbf{A} = \mathbf{0}$.

Boundary conditions have been derived by considering the actual structure of the junction.[4] Figure 1 shows the development of a junction system onto a 2D graphite sheet. We separate the development into three regions, the thick tube, the junction region, and the thin tube. We have a pair of a pentagon ($\mathbf{R}_5$) and heptagon ($\mathbf{R}_7$) ring, and $\mathbf{L}_5$ and $\mathbf{L}_7$ are the chiral vector of the thick and thin nanotube, respectively.

For metallic tubes, the boundary conditions are usual periodic boundary conditions and the solutions are a set of plane waves. In the vicinity of the Fermi energy, we have four conducting modes in tube regions: right- and left-going waves associated with K and K' points, respectively.

Boundary conditions take a different form in the junction region, where any point on the development moves onto the corresponding point after

making a rotation by $\pi/3$ around $\mathbf{R}$ as shown in Fig. 1. We have

$$\mathbf{F}[R_{\pi/3}\mathbf{r}] = T_{\pi/3}\,\mathbf{F}(\mathbf{r}),$$
$$T_{\pi/3} = \begin{pmatrix} 0 & 0 & 0 & \omega^{1/2} \\ 0 & 0 & -\omega^{-1/2} & 0 \\ 0 & -\omega^{-1/2} & 0 & 0 \\ \omega^{1/2} & 0 & 0 & 0 \end{pmatrix}, \tag{2.3}$$

where $\omega = \exp(2\pi i/3)$ and $R_{\pi/3}$ describes a $\pi/3$ rotation around $\mathbf{R}$. Because of the boundary conditions, states near the K and K' point mix together in the junction region. Figure 2 shows the topological structure of the junction system. Under these boundary conditions, the Schrödinger equation has solutions which are represented with Bessel J and Neumann functions N:

$$\mathbf{F}_{\mu}^{Z} = \frac{1}{\sqrt{L_5}} \begin{pmatrix} Z_{3\mu+1}(kr)e^{i(3\mu+1)\phi} \\ i\,\mathrm{sgn}(\varepsilon) Z_{3\mu+2}(kr)e^{i(3\mu+1)\phi} \\ (-)^{\mu} i\,\mathrm{sgn}(\varepsilon) Z_{3\mu+2}(kr)e^{i(3\mu+1)\phi} \\ (-)^{\mu} Z_{3\mu+1}(kr)e^{i(3\mu+1)\phi} \end{pmatrix}, \quad Z = J,\ N \tag{2.4}$$

with μ being an integer, $k = |\varepsilon|/\gamma$, and L_5 is the circumference of the thicker nanotube. In particular when the energy is equal to the Fermi energy ($\varepsilon = 0$), these solutions become:[4]

$$\mathbf{F}_{m}^{A} = \frac{1}{\sqrt{L_5}} \begin{pmatrix} 1 \\ 0 \\ 0 \\ (-1)^m \end{pmatrix} \left(\frac{+iz}{L_5}\right)^{3m+1},$$
$$\mathbf{F}_{m}^{B} = \frac{1}{\sqrt{L_5}} \begin{pmatrix} 0 \\ 1 \\ (-1)^{m+1} \\ 0 \end{pmatrix} \left(\frac{-i\bar{z}}{L_5}\right)^{3m+1}, \tag{2.5}$$

where m is an integer, $z = x + iy$, and $\bar{z} = x - iy$. We have chosen the origin at $\mathbf{R}$, the y axis in the direction of the axis of the thicker nanotube, and the x axis in the direction parallel to $\mathbf{L}_5$.

We put the right-going wave from the left side of the junction (through the thicker tube). To obtain the overall wave function of the system, we should connect these three types of solutions at the boundary $y = y_5$ (the line connecting $\mathbf{R}_5$ and $\mathbf{R}_5$–$\mathbf{L}_5$ in Fig. 1) and at $y' = y_7$ (the line connecting $\mathbf{R}_7$ and $\mathbf{R}_7 - \mathbf{L}_7$).

3. NUMERICAL RESULTS

In actual calculations, we have to limit the total number of eigenmodes in both nanotube and junction regions. In the junction region the wave

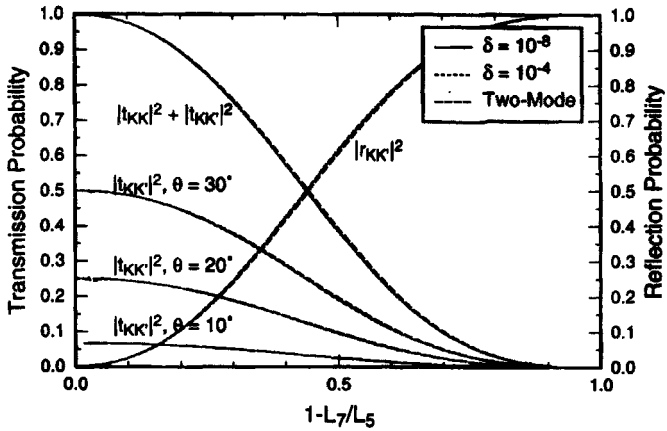

FIGURE 3 Calculated transmission and reflection probabilities versus the effective length of the junction region $(L_5-L_7)/L_5$. Contributions of intervalley scattering to the transmission are plotted for $\theta=10°$, 20°, and 30°. The results are almost independent of the value of δ.

function for $m \geq 0$ decays and that for $m<0$ becomes larger in the positive y direction. We shall choose cutoff M of the number of eigenmodes in the junction region, i.e., $-M-1 \leq m \leq M$, for a given value of L_7/L_5 in such a way that $(\sqrt{3}L_7/2L_5)^{3M} < \delta$, where δ is a positive quantity much smaller than unity. With the decrease of δ, the number of the modes included in the calculation increases.

Figure 3 shows some examples of calculated transmission and reflection probabilities for $\delta = 10^{-4}$ and 10^{-8}. An approximate expression for the transmission T and reflection probabilities R can be obtained by neglecting evanescent modes completely. The solution gives

$$\begin{aligned} T &= \frac{4L_5^3L_7^3}{(L_5^3+L_7^3)^2}, \quad T_{KK} = T\cos^2\left(\frac{3}{2}\theta\right), \quad T_{KK'} = T\sin^2\left(\frac{3}{2}\theta\right), \\ R &= \frac{(L_5^3-L_7^3)^2}{(L_5^3+L_7^3)^2}, \quad R_{KK} = 0, \qquad\qquad R_{KK'} = R, \end{aligned} \tag{3.1}$$

where the subscript KK means intravalley scattering within K or K' point and KK' stands for intervalley scattering between K and K' points. As for the reflection, no intravalley scattering is allowed. The dependence on the tilt angle θ originates from two effects. One is $\theta/2$ arising from the spinor-like character of the wave function in the rotation θ. Another θ comes from the junction wave function with $m=0$ which decays most slowly along the y axis. We have $T \sim 4(L_7/L_5)^3$ in the long junction $(L_7/L_5 \ll 1)$,

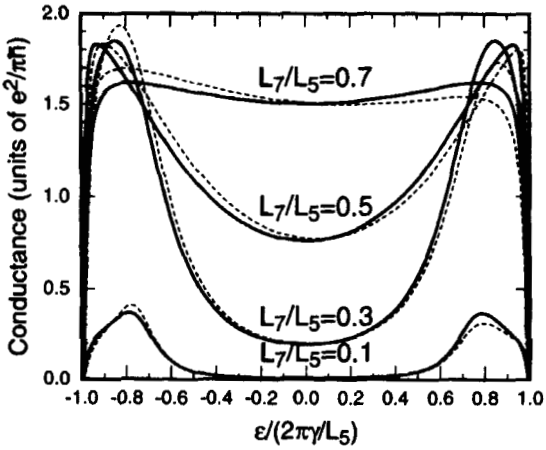

FIGURE 4 Calculated conductance versus the energy ε ($-2\pi/L_5 < \varepsilon/\gamma < +2\pi/L_5$) for various length of the junction ($L_7/L_5 = 0.7$, 0.5, 0.3, and 0.1 from top to bottom). Solid lines represent the results of the $\mathbf{k}\cdot\mathbf{p}$ method, while dashed lines show tight-binding data[5] for $L_5 = 50\sqrt{3}a$ (a is the lattice constant). The conductance grows with the energy and has a peak before the first band edge $\varepsilon/\gamma = \pm 2\pi/L_5$, followed by an abrupt falloff.

explaining results of numerical calculations in a tight-binding model quite well.[2]

As for the transmission, contributions from intervalley scattering ($K \to K'$) are plotted together for several values of θ. The dependence on the value of δ is extremely small and is not important at all, showing that the analytic expressions for the transmission and reflection probabilities obtained above are almost exact.

Figure 4 shows some examples of calculated transmission probabilities for energies lying between $-2\pi/L_5 < \varepsilon/\gamma < +2\pi/L_5$. Calculations were performed for various values of the length of the junction ($L_7/L_5 = 0.7$, 0.5, 0.3, and 0.1 from top to bottom). Solid lines represent the results of the $\mathbf{k}\cdot\mathbf{p}$ method, while dashed lines show tight-binding data[5] for $L_5 = 50\sqrt{3}a$ (a is the lattice constant). The tight-binding data are slightly deviated from those obtained by the $\mathbf{k}\cdot\mathbf{p}$ method, presumably due to size effects.

The conductance grows with the energy and has a peak before the first band edge $\varepsilon/\gamma = \pm 2\pi/L_5$. This behavior of conductance arises from the oscillatory feature of the Bessel and Neumann functions, which appear in the eigenmodes in the junction region as in Eq. (2.4).

Near the band edge, however, the conductance decreases abruptly and

falls off to zero. This behavior cannot be obtained if we ignore the evanescent modes in the tube region. This implies the formation of a kind of resonant state in the junction region, which would bring forth the total reflection into the thicker tube region. Detailed analysis of this mechanism is left for a future problem.

4. SUMMARY

We have studied the topology of a CN junction consisting of tubes with different circumferences L_5 and L_7 ($L_5 > L_7$). For a long junction and at $\varepsilon = 0$, the total conductance decays in proportion to $(L_7/L_5)^3$ as has been obtained in previous simulations.[2] The intervalley scattering contribution to the transmission coefficient grows as θ increases, where θ is the tilt angle between $\mathbf{L}_5$ and $\mathbf{L}_7$. The total conductance, however, stays almost same as that for $\theta = 0$. Energy dependence of the conductance was also calculated, which reflects the oscillatory behavior of wave functions in the junction region and exhibits an abrupt falloff near the band edge.

Acknowledgments

This work was supported in part by Grants-in-Aid for Scientific Research and for Priority Area, Fullerene Network, from Ministry of Education, Science and Culture, Japan. One of the authors (H.M.) acknowledges the support of a research fellowship of the Japan Society for the Promotion of Science for Young Scientists. Numerical calculations were performed in part on FACOM VPP500 in Supercomputer Center, Institute for Solid State Physics, University of Tokyo.

References

[1] S. Iijima, T. Ichihashi and Y. Ando, Nature (London) **356** (1992) 776.
[2] R. Tamura and M. Tsukada, Phys. Rev. B **55** (1997) 4991.
[3] H. Ajiki and T. Ando, J. Phys. Soc. Jpn. **62** (1993) 1255.
[4] H. Matsumura and T. Ando, J. Phys. Soc. Jpn. **67** (1998) 3542.
[5] T. Nakanishi, private communication.